from the more rapid elution, the chromatograms are very similar, with no obvious decrease in resolution at the faster flow rate. The loading factor was further examined, and Figure 8a (supplementary material) shows the effect of increasing the loading of $[Co(en)_2(Pro)]^{2+}$ on the normal analytical C_{18} column. Good peak resolution is maintained until 2500 nmol when the leading edge of the Δ ion becomes split into two. This effect has been described previously.[27] Further loading results in further splitting followed by peak broadening at 5120 nmol. With use of the RC column, good peak shape is maintained up to 25 600 nmol (14 mg) (Figure 8b (supplementary material)). A further increase results in peak broadening and a shorter retention time. Hence, for these complexes up to 10 times the loading can be accommodated with the RC column. Also, the peak splitting effect observed when the normal analytical column was used has been eliminated.

The maximum loading factor is also dependent on the retention time. Whereas only 2500 nmol of $[Co(en)_2(Pro)]^{2+}$ could be loaded onto the analytical C_{18} column before peak splitting occurred, as much as 6400 nmol of Δ,Λ-$[Co(en)_2(Ser(Bzl))]^{2+}$ could be loaded (Figure 8c) (supplementary material)).

Supplementary Material Available: Figures 5, 6, and 8, displaying chromatograms of β-$[Co(trien)(Ala)]^{2+}$ isomers, of a series of $[Co(trien)(AA)]^{2+}$ complex ions, and of the effect of increased sample loadings for $[Co(en)_2(Pro)]^{2+}$ and $[Co(en)_2(Ser(Bzl))]^{2+}$ (4 pages). Ordering information is given on any current masthead page.

Contribution from the Department of Chemistry,
Texas A&M University, College Station, Texas 77843

Generalized Molecular Orbital Calculations on the Ground and Ionic States of (η^4-Cyclobutadiene)tricarbonyliron(0)

JOHN W. CHINN, JR., and MICHAEL B. HALL*

Received September 8, 1982

Generalized molecular orbital calculations with configuration interaction are reported for $(\eta^4\text{-}C_4H_4)Fe(CO)_3$ and several of its low-lying ionic states. The results provide insight into the cyclobutadiene–metal bonding and suggest rather strong polarization of the six electrons in the cyclobutadiene–metal bond toward cyclobutadiene. Calculations on the ionic states resolve the longstanding discrepancy between the experimental assignments and the results of ab initio calculations. Differential electron correlation is shown to be important in determining the order of the low-lying ionic states.

Introduction

Cyclobutadiene (Cbd), which has intrigued chemists for more than a century, has been extensively studied theoretically, even though it has never been isolated experimentally.[1] Yet, these calculations have sought to establish the nature of both the ground-state geometry of this species (whether square or rectangular) and its electronic structure (whether singlet or triplet).[2] In 1956 Longuet-Higgins and Orgel suggested that Cbd might be stabilized by and isolated in complexes with transition-metal fragments, of which tricarbonyliron(0) was a likely candidate.[3] Over the next decade a number of transition-metal complexes containing substituted Cbd ligands were prepared[4] before Pettit and co-workers isolated the species proposed by Longuet-Higgins and Orgel, (η^4-cyclobutadiene)tricarbonyliron(0) (**1**).[5]

Although a solid-state structure of this complex has never been performed, a gas-phase electron diffraction study indicated that the Cbd ligand was square planar (D_{4h} symmetry)

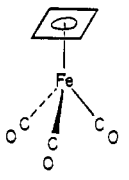

1

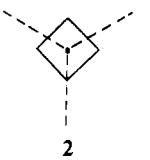

2

and periplanar to the $Fe(CO)_3$ fragment.[6b] A crystal structure on the tetraphenyl derivative of **1** revealed several interesting features: (1) the complex had the eclipsed conformation, **2**; (2) the C–C bond lengths were divided into two unequal sets, making the Cbd slightly diamond shaped; (3) the $Fe\text{–}C_{Cbd}$ distances were unequal; (4) the phenyl substitutes were displaced out of the Cbd plane away from the metal.[6a] These structural distortions were shown to be consequences of the interaction of the $Fe(CO)_3$ d_π orbitals with the Cbd p_π orbitals.[7]

Cyclobutadiene is considered to be antiaromatic according to the Hückel rules as it has only four π electrons.[8] However, when complexed to metal fragments—in particular, to $Fe(CO)_3$—it exhibits extraordinary reactivity of an electrophilic nature, much as benzene (an aromatic species) does.[9] This would indicate that **1** undergoes an internal transfer of electron density from the $Fe(CO)_3$ fragment to the Cbd ligand, which is then subject to attack by electrophiles.[10] That this might be a correct analysis has been demonstrated by the mass spectra of these compounds, which show the clear presence

(1) (a) Kekulé, A. *Justus Liebigs Ann. Chem.* **1872**, *162*, 77. (b) Baker, W.; McOmie, J. F. W. In "Non-Benzenoid Aromtic Compounds"; Ginsburg, D., Ed.; Wiley: New York, 1959; Chapter II. (c) Cava, M. P.; Mitchell, M. J. "Cyclobutadiene and Related Compounds"; Academic Press: New York, 1967. (d) C_4H_4 has been trapped in a low-temperature matrix; see: Masamue, S.; Souto-Bachiller, F. A.; Machiguchi, T.; Bertie, J. E. *J. Am. Chem. Soc.* **1978**, *100*, 4890.
(2) (a) Dewar, J. J. S.; Kohn, M. C.; Trinajstic, N. *J. Am. Chem. Soc.* **1971**, *93*, 3437. (b) Halevi, E. A.; Matsen, F. A.; Welsher, T. L. *Ibid.* **1976**, *98*, 7088. (c) Kollmar, H.; Staemmler, V. *Ibid.* **1977**, *99*, 3583. (d) Dewar, J. J. S.; Komornicki, A. *Ibid.* **1977**, *99*, 6174. (e) Borden, W. T.; Davidson, E. R.; Hart, P. *Ibid.* **1978**, *100*, 388. (f) Kollmar, H.; Carrion, F.; Dewar, M. J. S.; Bingham, R. C. *Ibid.* **1981**, *103*, 5292. (g) Borden, W. R.; Davidson, E. R.; Feller, D. *Ibid.* **1981**, *103*, 5725 and references therein.
(3) Longuet-Higgins, H. C.; Orgel, L. E. *J. Chem. Soc.* **1956**, 1969.
(4) See, for example: (a) Maitlis, P. M. *Adv. Organomet. Chem.* **1966**, *4*, 95. (b) Maitlis, P. M.; Eberius, K. W. In "Non-Benzenoid Aromatics"; Snyder, J. P., Ed.; Academic Press: New York, 1971; Chapter 6. (c) Pettit, R. *J. Organomet. Chem.* **1975**, *100*, 205. (d) Efraty, A. *Chem. Rev.* **1977**, *77*, 691 and references therein.
(5) Emerson, G. F.; Watts, L.; Pettit, R. *J. Am. Chem. Soc.* **1965**, *87*, 131.
(6) (a) Dodge, R. P.; Schomaker, V. *Acta Crystallogr.* **1965**, *18*, 614. (b) Davis, M. I.; Speed, C. S. *J. Organomet. Chem.* **1970**, *21*, 401.
(7) Chinn, J. W., Jr.; Hall, M. B. *J. Am. Chem. Soc.* **1983**, *105*, 4930.
(8) (a) Hückel, E. *Z. Phys.* **1931**, *70*, 204; (b) *Ibid.* **1931**, *71*, 310.
(9) (a) Fitzpatrick, J. D.; Watts, L.; Emerson, G. F.; Pettit, R. *J. Am. Chem. Soc.* **1965**, *87*, 3254. (b) Fitzpatrick, J. Ph.D. Dissertation, University of Texas, Austin, TX, 1970. (c) Pettit, R. *J. Organomet. Chem.* **1975**, *100*, 205.
(10) Bursten, B. E.; Fenske, R. F. *Inorg. Chem.* **1979**, *18*, 1760.

0020-1669/83/1322-2759$01.50/0

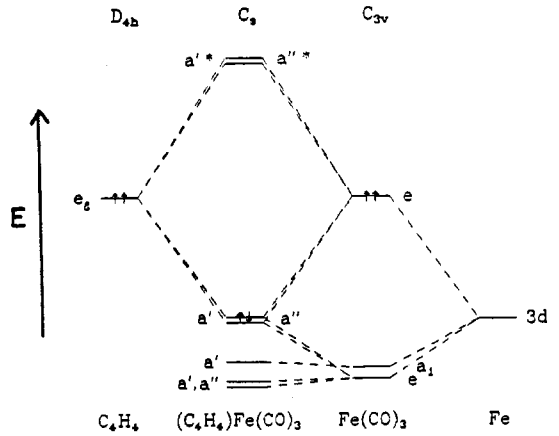

Figure 1. Simple qualitative molecular orbital diagram of the strongest fragment interactions in $(C_4H_4)Fe(CO)_3$.

of $C_4R_4Fe^+$ peaks and a noted absence of $C_4R_4^+$ peaks,[11] indicating the stabilizing ability of the metal on the Cbd ring.

Of special value in understanding the electronic structure of **1** is the use of ultraviolet photoelectron spectroscopy, which probes the valence orbitals of a compound.[12] These valence orbitals are very sensitive to shifts in electron density, and so a thorough understanding of their makeup would yield valuable information toward understanding the reactivity of **1**. The photoelectron spectrum (PES) of the complex was first recorded by Dewar and Worley in 1969.[13] The high-resolution work on **1** was later performed in 1975 by Hall et al., in which they conducted both He I and He II photoionization studies.[14] Yet, despite having been known for over a decade, the PES of **1** has never been completely and satisfactorily assigned.[14]

If we examine a simple molecular orbital diagram (Figure 1) of the interaction between $Fe(CO)_3$ and Cbd, we find that the highest occupied orbitals in the two fragments are energetically located to interact strongly with each other. Under C_s symmetry, this interaction produces a fully occupied bonding set (a'', a') and an unoccupied antibonding set (a'*, a''*) of orbitals. The other low-lying orbitals of $Fe(CO)_3$ carry over virtually unchanged into the complex. Thus, from this simple, qualitative diagram, we would expect two sets of ionizations in the PES: one group of three from primarily metal orbitals and one group of two from the strong mixing of the metal and Cbd orbitals. However, this simple analysis does not tell us either the ordering of these two groups or their energy separation. The metal levels could just as easily be above the metal–ligand set or be intermingled with them.

In the high-resolution PES of **1**, Hall et al. found two distinct ionization bands at low energy (8.45 and 9.21 eV), which were well separated from the next band cluster.[14] In the He I spectrum, the first band was less intense than the second, whereas the He II spectrum showed just the reverse: the first band was more intense than the second. In previous studies on other polyene–transition-metal complexes, the authors found that bands which increased in intensity relative to others on going from He I to He II ionization sources were due to photoionizations out of mainly localized metal d orbitals.[15] With this in mind, they assigned the first ionization (IP) as being due to the primarily metal nonbonding orbitals and the second as being due to the strongly interacting Fe–Cbd bonding orbitals.

The authors also performed a single-determinant, ab initio, Hartree–Fock–Roothaan (HFR) calculation[16] on **1** using a limited basis of Gaussian-type functions. Application of Koopmans' theorem[17] (KT) to the resulting orbital energies (1) gave an energy gap of 4.5 eV between the first two IP's, compared to the experimental value of 0.76 eV, (2) put both IP's too high in energy, and (3) predicted the first IP to be the bonding metal–Cbd band, in apparent contrast to the He II result. When the IP's were calculated by using total energy differences between the ground state and the ion (the ΔSCF method), they found that now the energy gap was too small (0.3 eV), both bands were too low in energy, and the ordering was still wrong. Therefore, both KT and ΔSCF have failed to properly interpret the observed PES of **1**.

Fenske–Hall molecular orbital (FHMO) calculations have also been reported for **1**.[10] In that study, the authors were primarily interested in the metal–Cbd interactions but reported the expected IP's based on Koopmans' theorem. Although the ordering was correct, the IP values and the band gap (1.75 eV) were much too large. These results are not unexpected. FHMO calculations have been consistently used to predict the correct ordering of PES ionization levels, even when the actual values have been too large.[18]

In this study, we will provide a description of the electronic structure of **1** at the post-Hartree–Fock level[19] and use it to calculate qualitatively correct values for the upper IP's and band gap. We will use a technique called generalized-molecular-orbital (GMO) theory[20] to generate an optimized set of primary orbitals for use in further configuration interaction (CI) studies. The procedure has been found to correctly order the IP's (which Hartree–Fock theory fails to do at times) and to produce improved IP values and band splittings. The potential utility of the GMO method for this study was demonstrated by the successful prediction of the correct order and energy splitting in the upper IP's of N_2.[21]

Theoretical Considerations

Generalized Molecular Orbital Theory. The GMO approach, which is detailed elsewhere,[20] uses a limited type of multiconfiguration self-consistent-field (MCSCF) calculation to provide an optimized set of primary orbitals for further CI studies, with only a modest additional effort and cost beyond that needed for the standard Hartree–Fock–Roothaan (HFR) molecular orbital (MO) approach.[16,22] In ordinary MO theory for a $2m$-electron, closed-shell molecule, the MO's are expanded in a linear combination of n basis functions which are often very similar to the atomic orbitals (AO's) of the constituent atoms. The total wave function in the HFR approach is a simple determinant of doubly occupied MO's. This results in the orbital space being divided into two shells, one of m doubly occupied orbitals and one of $n - m$ unoccupied orbitals:

(11) King, R. B.; Efraty, A. *Org. Mass Spectrom.* **1970**, *3*, 1233.
(12) (a) Turner, D. W.; Baker, C.; Baker, A. D.; Brundle, C. R. "Molecular Photoelectron Spectroscopy"; Wiley: New York, 1970. (b) Eland, J. H. D. "Photoelectron Spectroscopy"; Wiley: New York, 1974.
(13) Dewar, M. J. S.; Worley, S. D. *J. Chem. Phys.* **1969**, *50*, 654.
(14) Hall, M. B.; Hillier, I. H.; Connor, J. A.; Guest, M. F.; Lloyd, D. R. *Mol. Phys.* **1975**, *30*, 839.
(15) (a) Connor, J. A.; Derrick, L. M. R.; Hall, M. B.; Hillier, I. H.; Guest, M. F.; Higginson, B. R.; Lloyd, D. R. *Mol. Phys.* **1974**, *28*, 1193. (b) Guest, M. F.; Hillier, I. H.; Higginson, B. R.; Lloyd, D. R. *Ibid.* **1975**, *29*, 113.
(16) Roothan, C. C. J. *Rev. Mod. Phys.* **1951**, *23*, 69.
(17) Koopmans, T. *Physica (Amsterdam)* **1934**, *1*, 104.
(18) Fenske, R. F.; DeKock, R. L. *Inorg. Chem.* **1970**, *9*, 1053. (b) Lichtenberger, D. L.; Fenske, R. F. *Ibid.* **1974**, *13*, 486. (c) Fenske, R. F. *Prog. Inorg. Chem.* **1976**, *21*, 174. (d) Jensen, J. R. Ph.D. Thesis, University of Wisconsin, Madison, WI, 1978.
(19) Shavitt, I. "Methods of Electronic Structure Theory"; Schaefer, H. F., III, Ed.; Plenum Press: New York, 1977; Vol. III, Chapter 6.
(20) (a) Hall, M. B. *Int. J. Quantum Chem.* **1978**, *14*, 613. (b) Hall, M. B. *Chem. Phys. Lett.* **1979**, *61*, 461. (c) Hall, M. B. In "Recent Developments and Applications of Multiconfiguration Hartree-Fock Methods"; Dupuis, M., Ed.; National Technical Information Service: Springfield, VA, 1981; NRCC Proceedings No. 10, p 31.
(21) Hall, M. B. *Int. J. Quantum Chem., Quantum Chem. Symp.* **1979**, *No. 13*, 195.
(22) (a) Hartree, D. R. *Proc. Cambridge Philos. Soc.* **1928**, *24*, 89. (b) Fock, V. *Z. Phys.* **1930**, *61*, 126. (c) Roothaan, C. C. J. *Rev. Mod. Phys.* **1960**, *32*, 179.

$$(\phi...\phi_m)^2(\phi_{m+1}...\phi_n)^0 \quad (1)$$

Because of this partitioning by the wave function, the occupied orbitals are eigenfunctions of the same Fock operator and the variation principle is easily satisfied by employing the Roothaan procedure.[16]

In the GMO approach, each of these shells is further subdivided into two additional shells to generate an orbital space containing doubly occupied core orbitals (r shell), strongly occupied valence orbitals (t shell), weakly occupied valence-correlating orbitals (u shell), and unoccupied virtual orbitals (v shell):

$$(\phi_1...\phi_k)^2(\phi_{k+1}...\phi_l)^x(\phi_{l+1}...\phi_m)^y(\phi_{m+1}...\phi_n)^0 \quad (2)$$

A key feature of this technique is the fact that the orbitals are treated in shells, such that all the orbitals in a shell have equal occupation numbers and are eigenfunctions of the same Fock operator. It is this shell structure, with its similarity to standard MO theory, that suggested the use of the name generalized molecular orbital theory. As in HFR theory,[22c] the notation can be extended to open-shell systems, where one would have an additional set of singly occupied orbitals (s shell) with its own Fock operator.

The GMO wave function, which is consistent with the above partitioning scheme, can be written as

$$\Psi = (1 - n_t n_u \lambda^2)^{1/2}\psi_{00} + \lambda \sum_t \sum_u \psi_{tu} \quad (3)$$

where

$$\psi_{00} = |\phi_1\bar{\phi}_1...\phi_t\bar{\phi}_t...\phi_n\bar{\phi}_n| \quad (4)$$

$$\psi_{tu} = |\phi_1\bar{\phi}_1...\phi_u\bar{\phi}_u...\phi_n\bar{\phi}_n| \quad (5)$$

and n_t and n_u are the number of orbitals in the t and u shells, respectively. This wave function consists of a dominant single determinant (ψ_{00}), plus a correlation function ($\sum_t\sum_u\psi_{tu}$) that contains all determinants which can be constructed from paired double excitations from the strongly occupied t shell to the weakly occupied u shell, weighted equally by the variational parameter λ. For this wave function Ψ in the orbital space described, the occupation numbers of the t and u shells (x and y) will then be $2(1 - n_u\lambda^2)$ and $2n_t\lambda^2$, respectively. In the simple open-shell case with n_s orbitals, each containing one electron of the same spin, n_s singly occupied orbitals would be included in both ψ_{00} and ψ_{tu}.

The total electronic energy expression for this system can be written as

$$E = 2\sum_i f_i h_i + \sum_i \sum_j (a_{ij}J_{ij} + b_{ij}K_{ij}) \quad (6)$$

where h_i, J_{ij}, and K_{ij} are the usual one-electron, Coulomb, and exchange integrals, respectively. In standard MO theory $f_i = 1.0$, $a_{ij} = 2.0$, and $b_{ij} = -1.0$, while in a general MCSCF procedure those coefficients will depend on the individual orbital under consideration. The real advantage of the GMO method is that f_i, a_{ij}, and b_{ij} do not depend on the individual orbitals but only on the shell to which the orbitals belong. Because of this, the wave function and energy are independent of a unitary transformation of the orbitals within a shell and depend only on the mixing between shells. Thus, when the variational principle is used to minimize the energy (eq 6), the orbitals may be treated in groups (as they are in the standard HFR approach), allowing solution of the GMO problem by the usual SCF procedures.[16,22]

If the generalized coupling operator[23] is used to solve the problem, then the orbitals within each shell can be made canonical over any desired operator, and we will only need to construct three Fock-like operators for a closed-shell singlet (four operators for an open-shell doublet), and this will be true regardless of the size of the problem or the number of orbitals in each shell. Thus, the effort expended in solving the GMO equations is only 3 times that for the SCF part of the standard HFR approach, whereas the effort expended in solving MCSCF or generalized valence bond (GVB)[24] equations is roughly N times that for the standard HFR equations, where N is the number of noncore orbitals ($n_t + n_u$).

It must be pointed out that we do not expect the rather restricted GMO wave function (eq 3) to yield a very large fraction of the correlation energy; we use it simply as a means of defining the MO's for further CI calculations. Experience has shown that although the filled orbitals in a HFR calculations resemble the natural orbitals (NO's)[25] of extensive CI calculations, the unoccupied orbitals usually do not bear a similar resemblence. However, previous results for H_2O, N_2, BH_3, and B_2H_6 in large Gaussian basis sets did show that the GMO orbitals of both the t and u shells resembled the NO's of an all single- and double-excitation CI calculation. The similarity of the orbitals was reflected both in the overlap between the GMO's and the NO's[21] and in the correlation energies obtained with either set of orbitals.[26]

The orbital space for the ground-state GMO calculations was initially defined to be the seven orbitals illustrated in Figure 1 with the lower five filled orbitals making up the strongly occupied t shell and the upper two empty orbitals comprising the weakly occupied u shell. The orbital space for the ion calculations had the singly occupied orbitals in the s shell, the remaining four filled orbitals in the t shell, and either one or two of the empty orbitals in the u shell (if one of the u-set orbitals correlated the singly occupied orbital, it was removed from the calculation). This GMO space covered the MO's having the greatest percentage of iron 3d-orbital and Cbd $2p_\pi$-orbital character.

Configuration Interaction. Following determination of the GMO's of the ground state ($^1A'$) and the upper four ion states (giving two $^2A'$ and two $^2A''$ states), various amounts of CI were performed on the orbital space defined by the GMO procedure. This ranged from full CI, involving all possible spin- and symmetry-adapted configurations which can be constructed from the t, s, and u shells, to the allowance of only double excitations from the t to the u set. This was done to determine the most important configurations in both the ground and ion states and to examine their effects upon the ionization energies.

From the CI on the GMO's, one derives the natural orbitals (NO's) and their occupation numbers by diagonalization of the one-electron density matrix.[25] If we make the assumption that the same NO's and occupation numbers would be obtained from a GVB calculation[24] over this orbital space, then we can generate pseudo-generalized-valence-bond (PGVB) pairs in the following manner. If ϕ_1 and ϕ_2 are a strongly and weakly occupied pair of NO's from a CI calculation, the PGVB pairs, ϕ_a and ϕ_b, will be related to them by

$$N[(\phi_a(1))(\phi_b(2)) + (\phi_b(1))(\phi_a(2))] = C_1(\phi_1(1))(\phi_1(2)) - C_2(\phi_2(1))(\phi_2(2)) \quad (7)$$

where

$$\langle\phi_1|\phi_2\rangle = S_{12} = 0 \qquad \langle\phi_a|\phi_a\rangle = \langle\phi_b|\phi_b\rangle = S_{aa} = 1 \quad (8)$$

and

(23) (a) Hirao, K. *J. Chem. Phys.* **1974**, *60*, 3215. (b) Hirao, K.; Nakatsuji, H. *Ibid.* **1973**, *59*, 1457.

(24) Goddard, W. A., III; Dunning, R. H., Jr.; Hunt, W. J.; Hay, P. J. *Acc. Chem. Res.* **1973**, *6*, 368.

(25) (a) Lowdin, P.-O. *Phys. Rev.* **1955**, *97*, 1474. (b) Bingel, W. A.; Kutzelnigg, W. *Adv. Quantum Chem.* **1970**, *5*, 201. (c) Davidson, E. R. *Rev. Mod. Phys.* **1972**, *44*, 451.

(26) Taylor, T. E.; Hall, M. B. *J. Am. Chem. Soc.* **1980**, *102*, 6136.

$$S_{ab} = \langle \phi_a | \phi_b \rangle = \frac{C_1 - C_2}{C_1 + C_2} \neq 0 \tag{9}$$

whereby

$$N = (2 + 2S_{ab})^{-1/2} \tag{10}$$

From this, we find that

$$\phi_1 = \frac{\phi_a + \phi_b}{[2(1 + S_{ab})]^{1/2}} \qquad \phi_2 = \frac{\phi_a - \phi_b}{[2(1 - S_{ab})]^{1/2}} \tag{11}$$

and finally

$$\begin{aligned} \phi_a &= \left(\frac{C_1}{C_1 + C_2}\right)^{1/2} \phi_1 + \left(\frac{C_2}{C_1 + C_2}\right)^{1/2} \phi_2 \\ \phi_b &= \left(\frac{C_1}{C_1 + C_2}\right)^{1/2} \phi_1 - \left(\frac{C_2}{C_1 + C_2}\right)^{1/2} \phi_2 \end{aligned} \tag{12}$$

where the CI coefficients C_1 and C_2 are found from the occupation numbers:

$$C_1^2 + C_2^2 = \frac{n_1 + n_2}{2} = 1 \tag{13}$$

$$C_1 = (n_1/2)^{1/2} \qquad C_2 = (n_2/2)^{1/2} \tag{14}$$

Method. All computations were carried out on the Texas A&M University Amdahl 470V/6 and V/7 computers. The integral and HFR calculations were performed with the ATMOL2 system of programs,[27] while the GMO calculations were done with a program written by M. B. Hall. The CI calculations were performed with use of a package written for a Harris computer[28] and modified by T. E. Taylor and M. B. Hall for the Amdahl 470 computer.

The wave functions were then used in the program MOPLOT[29] to generate total electron density, $\rho(\mathbf{r})$, and orbital maps of regions of interest to aid in the interpretation of the interactions between the $Fe(CO)_3$ and Cbd fragments. The maps were drawn on a Versatec Model 1200 plotter using the program CONTOUR.[30] In the plots, solid lines represent positive density contours (the zero contour is the first solid one) and dashed lines represent negative contours. Adjacent contours of the same sign differ by a factor of 2 in all maps.

Geometry. Because no X-ray diffraction data were available for **1**, the molecular parameters for the calculations were chosen from examination of a number of related structures,[31] including the electron diffraction work of Davis and Speed on **1**.[6b] The Cbd fragment was given D_{4h} symmetry, and the $Fe(CO)_3$ fragment, C_{3v} symmetry. The molecule was fixed in the eclipsed conformation (**2**). The structural parameters are listed in Table I.

Basis. The basis functions employed in this study were obtained from a least-squares fit[32] of a linear combination of Gaussians to near-Hartree–Fock-quality Slater-type functions.[33] The program GEXP was used to process the functions from 1s outward, keeping each orbital of higher n quantum number orthonormal to the previous ones.[34] This procedure results in an efficiently nested representation of the function. The number of Gaussians used for each function was increased until the integral error of the fit[32] was less than 6×10^{-4}. It was determined that three Gaussians per atomic orbital were sufficient except for carbon and oxygen 2p, where four Gaussians were used, and iron 3d, where five were used.

In the molecular calculations, the most diffuse components of Cbd carbon 2p and of iron 3d were split off to form double-ζ representations. Since we were principally interested in studying the Cbd–Fe interactions the carbonyl carbon and oxygen 2p functions were kept fully contracted. Experience has shown that this is a good approximation for those parts of a molecule not under close scrutiny. The iron basis was also augmented by a single exponent of 0.20 for the 4s function and a single exponent of 0.25 for the 4p. The hydrogen 1s was fit to an exponent of 1.2.[35]

Table I. Structural Parameters Used in the Calculations on $(C_4H_4)Fe(CO)_3$[a]

parameter	value	parameter	value
r_{C-C}, Å	1.437[b]	r_{C-O}, Å	1.137[d]
r_{Fe-CH}, Å	2.065[c]	∠OC-Fe-CO, deg	98[d]
r_{Fe-CO}, Å	1.793[d]	∠Fe-C-O, deg	180[e]

[a] Bond lengths are in Å. [b] Reference 31b. [c] Reference 6. Value based on the average of the two structures. [d] Reference 31a. Values based on an average of many structures. [e] Idealized; actual value is close to 179°.

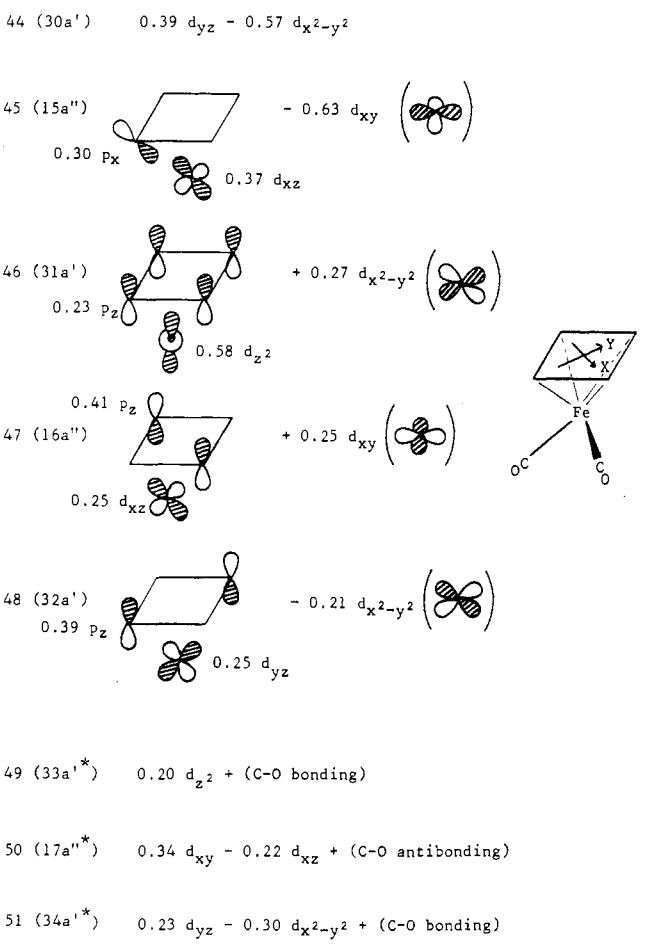

Figure 2. Character of the upper molecular orbitals for $(Cbd)Fe(CO)_3$ from the closed-shell HFR calculation on the ground state.

(27) Hillier, I. H.; Saunders, V. R. "ATMOL2 System"; Chemistry Department, University of Manchester: Manchester, England.
(28) Written by C. T. Corcoran, J. M. Norbeck, and P. R. Certain of the Chemistry Department, University of Wisconsin, Madison, WI.
(29) Lichtenberger, D. L. Ph.D. Dissertation, University of Wisconsin, Madison, WI, 1974. Program available from: Quantum Chemistry Program Exchange, Indiana University, Bloomington, IN 47401; Program 284.
(30) An in-house program that uses CONREC, a special smoothing routine for drawing contours, developed at the National Center for Atmospheric Research (NCAR), Boulder, CO, and adapted for use on the Amdahl 470V/6 by Thomas Reid, Data Processing Center, Texas A&M University.
(31) (a) Davis, R. E.; Riley, P. E. *Inorg. Chem.* **1980**, *19*, 674. (b) Riley, P. E.; Davis, R. E. *J. Organomet. Chem.* **1976**, *113*, 157.
(32) Stewart, R. F. *J. Chem. Phys.* **1970**, *52*, 431.
(33) (a) Clementi, E. *J. Chem. Phys.* **1964**, 40. (b) Clementi, E. *IBM J. Res. Dev.* **1965**, *9*, 2; and its supplement, "Tables of Atomic Functions".
(34) Hall, M. B. Ph.D. Dissertation, University of Wisconsin, Madison, WI, 1972.

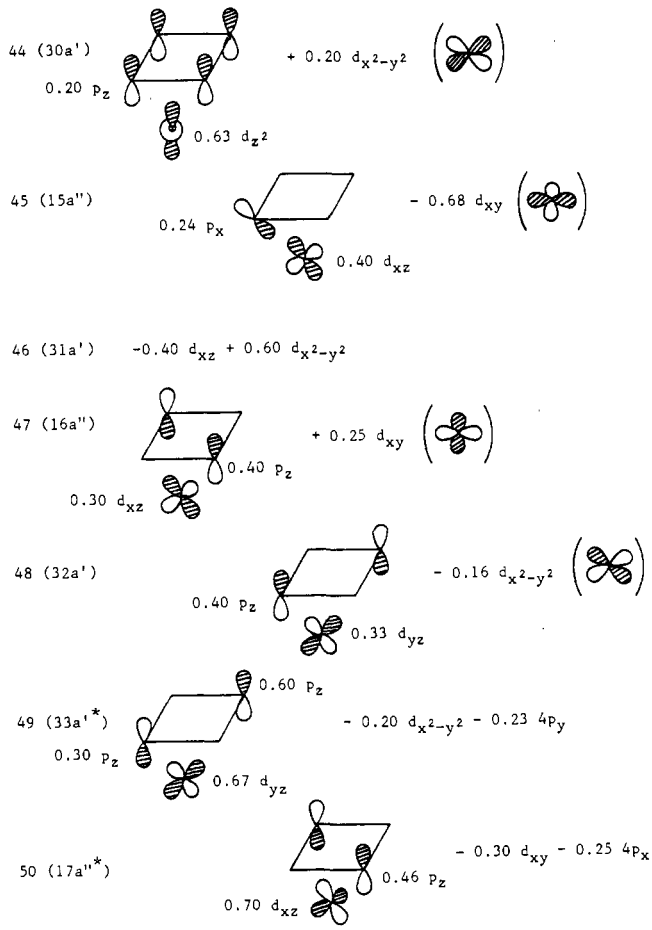

Figure 3. Character of the upper molecular orbitals for (Cbd)Fe(CO)$_3$ from the four-orbital GMO calculation on the ground state.

Results and Discussion

Ground State. Convergence of the Hartree–Fock equation led to a set of molecular orbitals (Figure 2) from which to choose our GMO space. Clearly, 30a′, 15a″, and 31a′ are primarily metal lone pair in character, although 31a′ involves d_{z^2} bonding with the Cbd a_{2u} combination of carbon p_π orbitals. The strongly mixed set of orbitals (metal–ligand bonding), 16a″ and 32a′, did not have any obvious components in the virtual space that were antibonding counterparts. So, two orbitals of the proper symmetry (17a″* and 34a′*) were chosen as the weakly occupied *u* set for the strongly occupied *t* set, 16a″ and 32a′. (It is important to note here that the asterisk will denote both virtual (*v* set) and weakly occupied (*u* set) orbitals.) The GMO calculation was converged in this limited, four-orbital space to give the GMO's in Figure 3. Notice that the new 33a′* and 17a″* orbitals are now the correlated antibonding metal–ligand set for the bonding combination, 16a″ and 32a′.

Full CI was performed over this set of four orbitals to generate the natural orbitals. A larger CI calculation was also run which included 30a′, 31a′, and 34a′*. The resulting total energies are listed in Table II. Table III contains the most important configurations for the level of CI run and the coefficients of these configurations in the CI wave function. The NO occupation numbers for the ground state are tabulated in Table IV. We expect to find (and do) that the addition of three more orbitals to the starting four-orbital space changed the CI wave function very little. The principal configurations in this larger CI space (Table III), which account for nearly 99% of the CI wave function, were the same principal ones in the smaller space. Hence, we shall confine ourselves to discussing calculations with this smaller set.

(35) Hehre, W. J.; Stewart, R. F.; Pople, J. A. *J. Chem. Phys.* **1969**, *51*, 2657. The value used represents the best average for hydrogen for all but the most polar bonding situations.

Table II. Calculated Total Energies (in au) for the Ground and Ion States of $(C_4H_4)Fe(CO)_3$

states	energy
Ground State	
^{1}A′ (HFR)	−1737.709 022
^{1}A′ (GMO)	−1737.728 069
^{1}A′ (CI-260 configns)	−1737.777 674
^{1}A′ (CI-12 configns)	−1737.758 900
Ion States	
^{2}A″ = (16a″)^1 (GMO)	−1737.476 244
^{2}A″ = (16a″)^1 (CI-10 configns)	−1737.478 908
^{2}A″ = (15a″)^1 (GMO)	−1737.483 280
^{2}A″ = (15a″)^1 (CI-39 configns)	−1737.554 083
^{2}A″ = (15a″)^1 (CI-11 configns)	−1737.543 421

Table III. Most Important Configurations from the GMO-CI Calculation of $(C_4H_4)Fe(CO)_3$ over Several Orbital Spaces in the Ground State (^{1}A′)

config[a]	CI coeff
(1) Starting Orbital Space: (30a′)^2(31a′)^2(16a″)^2(32a′)^2(33a′*)^0(17a″*)^0(34a′*)^0 (260 Possible Configurations)	
(A)(16a″)^2(32a′)^2	0.9554
(A)(32a′)^2(17a″*)^2	−0.1449
(A)(16a″)^1(32a′)^1(33a′*)^1(17a″*)^1 × $\alpha\beta\alpha\beta$	−0.1338
(A)(16a″)^2(33a′*)^2	−0.1387
(A)(16a″)^1(32a′)^1(33a′*)^1(17a″*)^1 × $\alpha\alpha\beta\beta$	0.1284
(A)(16a″)^1(32a′)^1(17a″*)^1(34a′*)^1 × $\alpha\alpha\beta\beta$	0.0527
(A)(16a″)^2(34a′*)^2	−0.0520
(2) Starting Orbital Space: (16a″)^2(32a′)^2(33a′*)^0(17a″*)^0 (12 Possible Configurations)	
(16a″)^2(32a′)^2	0.9676
(32a′)^2(17a″*)^2	−0.1520
(16a″)^1(32a′)^1(33a′*)^1(17a″*)^1 × $\alpha\beta\alpha\beta$	−0.1437
(16a″)^2(33a′*)^2	−0.1366
(16a″)^1(32a′)^1(33a′*)^1(17a″*)^1 × $\alpha\alpha\beta\beta$	0.1236

[a] (A) = (30a′)^2(31a′)^2.

As can be seen in Table III, the main configurations involve split- and paired-double excitations from the ground-state bonding orbitals to their antibonding counterparts. These few configurations account for only 5% of the wave function, but it is this small fraction of the total energy (50 millihartrees or about 31 kcal/mol) which is responsible for important features in the spectroscopy and chemistry. Thus, the *u* set of orbitals is allowing the electrons of the *t* set to move apart into different regions in the molecule; this is what is meant by correlation.

We can describe this in another way by taking the NO occupation numbers (Table IV) and constructing pseudo-GVB (PGVB) orbitals by using these numbers to compute PGVB coefficients. This will produce symmetric and antisymmetric combinations of the four principal orbitals, and each of these GVB-like orbitals will contain one electron. The NO's before combination are shown in Figure 4, and the PGVB pairs, in Figure 5. For the a″ NO's (Figure 4) we see that we have strongly bonding and antibonding p_π–d_{xz} interactions. In the PGVB description (Figure 5) each orbital is filled with one electron which can freely move about its own space. In this case, one electron occupies a strongly metal–ligand bonding orbital, while the other electron occupies primarily a Cbd-localized orbital. So, only one electron of the pair is responsible for bonding the Cbd to the iron. The other remains mostly on the ring, enhancing the electron density there and, consequently, enhancing the polyene's susceptibility to electrophilic attack. The same process occurs with the a′ orbitals.

Table IV. Natural Orbital Occupation Numbers for the Ground (^{1}A′) and Ion (^{2}A″) States for $(C_4H_4)Fe(CO)_3$ at Various Levels of CI

	30a′	15a″	31a′	16a″	32a′	33a′*	17a″*	34a′*
(^{1}A′) (260 configns)	1.9980	2.0	1.9858	1.9175	1.9196	0.0757	0.0784	0.0244
(^{1}A′) (12 configns)	2.0	2.0	2.0	1.9298	1.9402	0.0602	0.0698	0
(^{2}A″) = (16a″)^1 (10 configns)	2.0	2.0	2.0	0.9982	1.9040	0.0960	0.0018	0
(^{2}A″) = (15a″)^1 (11 configns)	2.0	1.0	2.0	1.8761	1.8718	0.1282	0.1239	0
(^{2}A″) = (15a″)^1 (39 configns)	2.0	1.0036	2.0	1.8580	1.8582	0.1419	0.1384	0

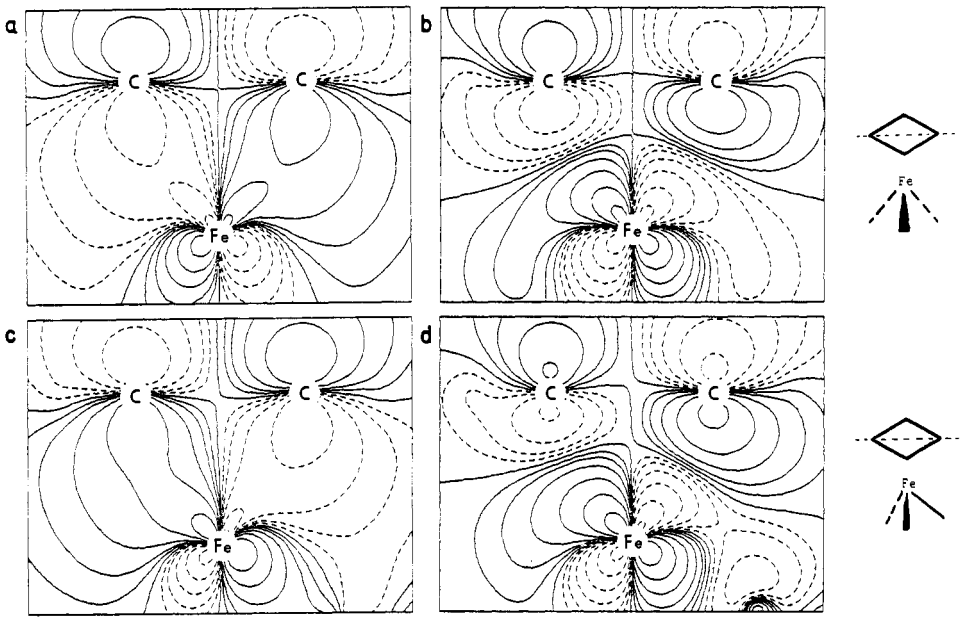

Figure 4. CI natural-orbital plots in the vertical *xz* (maps a and b) and *yz* (maps c and d) planes of $(Cbd)Fe(CO)_3$. Map a is 16a″, map b is 17a″, map c is 32a′, and map d is 33a′*.

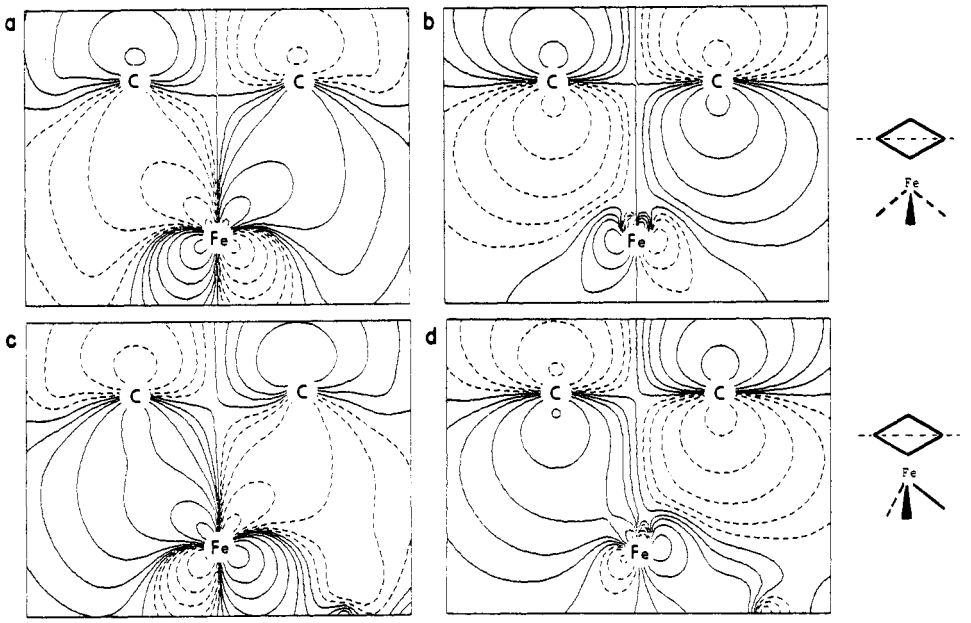

Figure 5. PGVB orbital plots of the orbital pairs constructed from the NO's shown in Figure 4. One electron is in each of these orbitals. Map a is the PGVB sum of 16a″ and 17a″*, while map b is the difference of those orbitals (with PGVB coefficients 0.9166 and 0.3997). Map c is the PGVB sum of 32a′ and 33a′*, while map d is their difference (with PGVB coefficients 0.9220 and 0.3871).

It is worth noticing that, in the strongly occupied 32a′ orbital (Figure 4), the largest contours occur between the iron and the carbon trans to the eclipsing carbonyl. It is this orbital that is primarily responsible for shortening the trans-$Fe–C_{Cbd}$ bond in the structure of the tetraphenyl derivative of **1**. Also, because the Cbd retains nearly two electrons in localized PGVB orbitals and strongly shares the other two with the metal, we can understand how the Cbd would appear to be nearly aromatic (approaching a six-π-electron configuration) in its reactivity.[9] Indeed, this picture describes better the "metalloaromatic" character which Bursten and Fenske ascribed to **1**.[10] Simply stated, a charge transfer has occurred, with the $Fe(CO)_3$ shifting electron density into the Cbd framework. Because of this, the Cbd is calculated to have almost a 1– charge (0.87–).

Ion States and PES. Using this wave function, which seems to account for the structure and reactivity of **1**, we reinvestigated the PES of the complex to see if we could calculate the correct IP's for the upper bands. Since there will be a′ and a″ ionizations occurring out of both the metal and met-

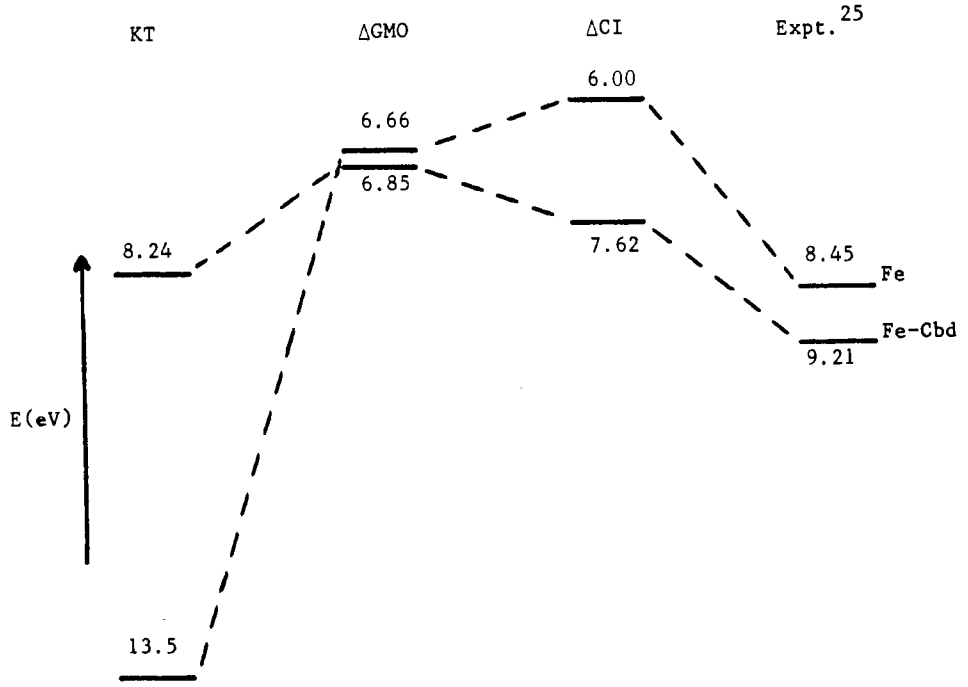

Figure 6. Comparison of the calculated IP's for $(Cbd)Fe(CO)_3$ from this study with the experimental work of Hall et al.[14]

al–ligand orbital groups (see Figure 1), we will discuss the IP's in terms of the a″ orbitals. An equivalent description will explain the a′ ionizations.

The GMO wave function was reconverged for each of two doublet states, $(15a'')^1$ and $(16a'')^1$, with use of five- and three-orbital spaces, respectively. (Since 16a″ was singly occupied, its correlating orbital, 17a″*, was removed from the starting *u* space.) Full CI was performed on the resulting GMO wave functions. The NO occupation numbers and most important configurations for these ion states are given in Tables IV and V, and the total energies, in Table II. It is important to realize that, in order to correctly calculate the IP's from the differences in CI energies, one must ensure that both the ground- and ion-state CI wave functions match as nearly as possible. Thus, one needs to keep both the number and the type of configurations similar in the two wave functions. This will avoid errors caused by one wave function having more correlation (and a lower energy) than the other. With this in mind, the full CI (39 configurations) for the $^2A''$ state, resulting from ionization out of the 15a″ orbital, was not used in the IP configuration. Rather, a subset of configurations (11), in which 15a″ was kept singly occupied and all remaining configurations having only a single excitation were removed, gave a configuration space which matched very well the four-orbital ground-state space (12 configurations).

With use of these total energies, the IP values for ionization from the 15a″ and 16a″ orbitals were calculated and are graphed in Figure 6. It is most important to realize that, whereas ΔSCF calculations[14] did *not* correctly order the IP's, the GMO calculations did, albeit with too small an energy splitting (0.19 eV compared to the experimental value of 0.76 eV[14]). Thus, the small additional correlation that the limited MCSCF-type GMO calculation has introduced (with a very small orbital space) is enough to give the correct ordering. The CI values increase the differential correlation and the splitting, but the IP's are too small and the splitting is too large (1.62 eV).

The nature of these ionic states is significantly different from those reported in recent Xα–SW calculations.[36] According to the Xα–SW calculations the molecular orbitals of the ions are very similar to those of the molecule. However, according to the GMO–CI calculations, when one removes an electron from 15a″ (Fe), the remaining electron localizes by increasing its $3d_{xy}$ character and decreasing its C character almost to zero. This dramatic change in character provides some of the relaxation energy which is one of the primary reasons these mainly Fe ionizations occur at a low IP. When an electron is removed from 16a″ (Fe–Cbd) the remaining electron becomes more delocalized. The 16a″ orbital loses $3d_{xz}$ character and gains C character. The same trends are observed in the

Table V. Most Important Configurations from the GMO–CI Calculations of the $(C_4H_4)Fe(CO)_3$ Ion States ($^2A''$) in Several Orbital Spaces

confign	CI coeff
(1) Starting Orbital Space for the $^2A''$ State Obtained by Ionization out of the 16a″ Orbital: $(32a')^2(16a'')^1(33a'^*)^0(17a''^*)^0$ (10 Possible Configurations)	
$(32a')^2(16a'')^1$	0.9742
$(16a'')^1(33a'^*)^2$	−0.2145
$(32a')^1(16a'')^1(33a'^*)^1 \times \alpha\alpha\beta$	−0.0456
$(32a')^1(33a'^*)^1(17a''^*)^1 \times \alpha\alpha\beta$	0.0409
(2) Starting Orbital Space for the $^2A''$ State Obtained by Ionization out of the 15a″ Orbital: $(32a')^2(16a'')^2(15a'')^1(33a'^*)^0(17a''^*)^0$ (39 Possible Configurations)	
$(32a')^2(16a'')^2(15a'')^1$	0.9067
$(16a'')^2(15a'')^1(33a'^*)^2$	−0.2004
$(32a')^2(15a'')^1(17a''^*)^2$	−0.1972
$(32a')^2(16a'')^1(15a'')^2$	−0.1683
$(32a')^2(16a'')^1(15a'')^1(17a''^*)^1 \times \alpha\beta\alpha\beta\alpha$	0.1334
$(32a)^1(16a'')^2(15a'')^1(33a'^*)^1 \times \alpha\alpha\beta\beta\alpha$	−0.1195
$(32a)^1(16a'')^1(15a'')^1(33a'^*)^1(17a''^*)^1 \times \alpha\alpha\alpha\beta\beta$	−0.1146
$(32a)^1(16a'')^1(15a'')^1(33a'^*)^1(17a''^*)^1 \times \alpha\beta\alpha\beta\alpha$	0.0817
$(15a'')^1(33a'^*)^2(17a''^*)^2$	0.0775
$(32a)^1(16a'')^1(15a'')^1(33a'^*)^1(17a''^*)^1 \times \alpha\beta\alpha\alpha\beta$	−0.0752
(3) Orbital Space as in (2) but with 15a″ Kept Singly Occupied and All Configurations Having Only One Single Excitation Removed (11 Possible Configurations)	
$(32a')^2(16a'')^2(15a'')^1$	0.9388
$(16a'')^2(15a'')^1(33a'^*)^2$	−0.2044
$(32a')^2(15a'')^1(17a''^*)^2$	−0.1991
$(32a')^1(16a'')^1(15a'')^1(33a'^*)^1(17a''^*)^1 \times \alpha\alpha\alpha\beta\beta$	−0.1248
$(15a'')^1(33a'^*)^2(17a''^*)^2$	0.0859
$(32a')^1(16a'')^1(15a'')^1(33a'^*)^1(17a''^*)^1 \times \alpha\beta\alpha\beta\alpha$	0.0707
$(32a')^1(16a'')^1(15a'')^1(33a'^*)^1(17a''^*)^1 \times \alpha\beta\alpha\alpha\beta$	−0.0695

(36) Kostič, N. M.; Fenske, R. F. *Chem. Phys. Lett.* **1982**, *90*, 306.

Xα-SW calculation, but the spherical averaging of the potential in these calculations prevents them from displaying their full effect.

Conclusions

Although the small basis set and limited CI precludes accurate values for the IP's, we have shown that some account of the differential correlation energy may be necessary before the correct order of the ionic states is obtained. The inversion of the order of the ionic states compared to that predicted by KT occurs for two reasons. First, the IP of the mainly metal d electrons is predicted to be too large because KT fails to account for the large shielding provided by these compact d orbitals.[37] Thus, there is a huge reduction in the predicted IP of these electrons at the ΔSCF level. Second, there is a substantial differential correlation energy between the two types of ionic states. In the molecule the highly delocalized metal-Cbd electrons are not as well described by the simple MO formalism as are the localized metal electrons. The loss of this near-degenerate type of correlation when a hole is created in the delocalized metal-Cbd orbitals gives rise to an increase in the predicted IP. The differential correlation effects are overestimated by our procedure because the CI was designed primarily to correlate the electrons in the metal-Cbd bonds. The ground state of $(\eta^4\text{-}C_4H_4)Fe(CO)_3$ at the CI level provides insight into the nature of the cyclobutadiene-metal interaction and correctly accounts for the aromatic character of the metal-bound cyclobutadiene, the nucleophilic character of the Cbd ring, and the tilt of the ring system.

Acknowledgment. This work was supported by the National Science Foundation (Grant No. CHE 79-20993) and the Robert A. Welch Foundation (Grant No. A-648).

Registry No. 1, 12078-17-0.

(37) Calabro, D. C.; Lichtenberger, D. L. *Inorg. Chem.* **1980**, *19*, 1732.

Contribution from the Christopher Ingold Laboratories, University College London, London WC1H 0AJ, U.K.

On the Nature of the Sulfur Chromophores in Ultramarine Blue, Green, Violet, and Pink and of the Selenium Chromophore in Ultramarine Selenium: Characterization of Radical Anions by Electronic and Resonance Raman Spectroscopy and the Determination of Their Excited-State Geometries

ROBIN J. H. CLARK,* TREVOR J. DINES, and MOHAMEDALLY KURMOO

Received January 4, 1983

By a combination of electronic and resonance Raman spectroscopy, it is shown that the key chromophores in ultramarine green are S_3^- and S_2^- and that various forms of ultramarine violet as well as ultramarine pink contain S_3^- and S_2^- together with a third chromophore, not certainly characterized. This last species, for which λ_{max} = 520 nm, predominates in all the violet and pink forms, especially in the latter. Ultramarine selenium, which is brick red (λ_{max} = 490 nm), readily yields a single long progression (to 13 members) under resonance Raman conditions; the progression is identified as arising from the Se_2^- ion, for which the following spectroscopic constants were established: $\omega_e = 329.6 \pm 0.3$ cm^{-1}, $\omega_e x_e = 0.70 \pm 0.03$ cm^{-1}. Excitation profiles of all resonance-enhanced bands have been measured and fitted to a Franck-Condon model for the intensity of the scattering. From the best fit between calculated and observed excitation profiles, values for the change in the equilibrium S-S and Se-Se bond lengths on excitation to the resonant excited state in each case were calculated to be 0.30 ± 0.01 and 0.32 ± 0.02 Å, respectively.

Introduction

The nature of the species responsible for the blue color formed ($\lambda_{max} \simeq 600$ nm, $\epsilon_{max} \simeq 10^4$ M^{-1} cm^{-1}) when alkali metal polysulfides are dissolved in donor solvents such as dimethylformamide or hexamethylphosphoramide has recently been established[1] to be the radical anion S_3^-. No salts of this anion have ever been prepared, owing to the very rapid dimerization of the ion when usually appropriate counterions are added to its solutions. The same species has been identified as being responsible for the deep blue color of sulfur dissolved in a LiCl-KCl eutectic, in CsCl-$AlCl_3$ or KNCS melts, in the aluminosilicate mineral lapis lazuli, and in its synthetic equivalent ultramarine blue.[2-5] The last is an important chemical in the pigment industry, owing to the richness and durability of its royal blue color. Small quantities of the S_2^- ion (λ_{max} = 380-400 nm) have also been shown to be present in ultramarine blue.[1] Ultramarine green has been shown to contain the same two chromophores as the blue but in more nearly comparable proportions.[1]

By modification to the preparative procedures it is possible to make various shades of ultramarine violet, as well as ultramarine pink (or red). The nature of the species present in these forms of ultramarine is not fully understood, nor is it known whether the proportions of the chromophores change continuously or stepwise from one shade of ultramarine to another.

It has, moreover, been known since the 1920s that selenium can replace sulfur in ultramarine with only minor changes to the aluminosilicate framework and that selenium can also replace sulfur in "boron" ultramarine with the formation of pink to brown colors.[6-8] The nature of the selenium-containing

(1) Clark, R. J. H.; Cobbold, D. G. *Inorg. Chem.* **1978**, *17*, 3169. Seel, F.; Güttler, H. J. *Angew. Chem., Int. Ed. Engl.* **1973**, *12*, 420.
(2) Holzer, W.; Murphy, W. F.; Bernstein, H. J. *J. Mol. Spectrosc.* **1969**, *32*, 13.
(3) Clark, R. J. H.; Franks, M. L. *Chem. Phys. Lett.* **1975**, *34*, 69.
(4) Chivers, T. In "New Uses of Sulfur"; West, J. R., Ed.; American Chemical Society: Washington DC, 1975; Adv. Chem. Ser. No. 140, pp 499-537.
(5) Berg, R. W.; Bjerrum, N. J.; Papatheodorou, G. N.; Von Winbush, S. *Inorg. Nucl. Chem. Lett.* **1980**, *16*, 201.

0020-1669/83/1322-2766$01.50/0